Research article

Prognostic model and ceRNA network of m7G- and radiosensitivity-related genes in hepatocellular carcinoma

Miaowen Liu [a,1], Meiyan Zhu [a,1], Yingxiong Huang [b,1], Jian Wu [c,***],
Zhenwei Peng [a,**], Ying Liang [d,*]

[a] Department of Radiation Oncology, The First Affiliated Hospital, Sun Yat-sen University, Guangzhou, 510080, China
[b] Department of Emergency, the First Affiliated Hospital, Sun Yat-sen University, Guangzhou, 510080, China
[c] Center of Hepato-Pancreato-Biliary Surgery, The First Affiliated Hospital, Sun Yat-sen University, Guangzhou, Guangdong Province, 510080, China
[d] Department of Nephrology, Guangzhou Eighth People's Hospital, Guangzhou Medical University, China

A B S T R A C T

Background: Radiotherapy is an effective treatment for hepatocellular carcinoma (HCC). Recent studies indicated that N7-methylguanosine (m7G)-associated genes are involved in radio-resistance and prognosis of HCC. However, the prognostic value and underlying mechanism of m7G-and radiosensitivity-associated genes are still lacking.
Methods: The related statistics of HCC were downloaded from The Cancer Genome Atlas (TCGA). M7G- and radiosensitivity-associated genes were screened and evaluated using correlation, differential, univariate, and multivariate analysis. The least absolute shrinkage and selection operator (LASSO) algorithm was used to establish a prognostic model. Prognostic efficacy, functional analysis, immune cell infiltration, and drug sensitivity of the prognostic model were assessed. The ceRNA network was predicted and evaluated through the StarBase database, correlation analysis, expression analysis, and survival analysis.
Result: METTL1, EIF3D, NCBP2, and WDR4 participated in prognosis model construction. The favorable prediction efficiency has been verified in both the training and verification sets. Different risk groups have differences in prognosis outcome, function analysis, immune cell infiltration, and drug sensitivity. NCBP2 can be used to predict the prognosis and has excellent potential in immunotherapy. A prognostic ceRNA network based on the NCBP2/miR-122-5p axis was established.
Conclusion: The prognosis model of m7G- and radiosensitivity-related genes is constructed, and widely used in clinical prognosis, immunotherapy, and drug therapy. NCBP2, as a hub gene, may be a prognostic biomarker for HCC and is related to immunotherapy. Establishing the NCBP2/miR-122-5p axis helps study the mechanism of ceRNA and provides new ideas for finding a new candidate biomarker.

* Corresponding author. No.627 Dongfeng East Road, Guangzhou, 510060, China.
** Corresponding author. Department of Radiation Oncology, The First Affiliated Hospital, Sun Yat-sen University, NO.58 Zhongshan Road II, Guangzhou, 510080, China.
*** Corresponding author. Center of Hepato-Pancreato-Biliary Surgery, The First Affiliated Hospital, Sun Yat-sen University, NO.58 Zhongshan Road II, Guangzhou, 510080, China.
E-mail addresses: wujian3@mail.sysu.edu.cn (J. Wu), pzhenw@mail.sysu.edu.cn (Z. Peng), gz8hliangying@yeah.net (Y. Liang).
[1] Miaowen Liu, Meiyan Zhu, and Yingxiong Huang contributed equally to this work.

1. Introduction

Liver cancer accounts for a death rate of 8.3 % of malignancies, with an estimated 0.83 million deaths worldwide in 2020 [1]. Meanwhile, the incidence of hepatocellular carcinoma (HCC) in primary liver cancer is as high as 90 % [2,3]. HCC is associated with viral infection, alcohol, diabetes, and other biochemical factors [4–6]. A novel and more precise prognostic biomarker and the latent regulatory mechanisms of prognostic factors are still the goals that need to be broken through [7].

Radiation therapy is considered an effective remedy for early-stage HCC, but its effectiveness is limited [8]. Exploring the regulatory mechanisms related to radiosensitivity and improving radiosensitivity have also become a focus of clinical attention [9,10]. N7-methylguanosine (m7G), an increasingly acquainted RNA modification, is involved in the cancer development [11]. METTL1 is a well-known m7G regulator, which not only participates in cell cycle and angiogenesis of HCC but also in radioresistance and drug resistance of HCC [12–14]. However, the relationship between the m7G and radiosensitivity remains ambiguous, and the underlying mechanism between them is of great value for exploration.

In this study, we screened m7G- and radiosensitivity-associated genes and selected intersectional genes with differential expression and prognostic value to construct a prognostic model. Prognostic efficacy, functional analysis, immune cell infiltration, and drug sensitivity of the prognostic model were assessed. At the same time, we screened the hub gene among the intersection genes, explored its clinical value, upstream microRNA (miRNA), and long noncoding RNA (lncRNA), and constructed the competing endogenous RNA (ceRNA) regulatory network.

2. Materials and methods

The design process of the entire study is displayed in Supplementary Figure S1. M7G- and radiosensitivity-related genes were identified, and a suitable prognosis model was constructed. Prognostic efficacy, functional analysis, immune cell infiltration, and drug sensitivity of the prognostic model were evaluated. NCBP2 was identified as the hub gene. The prognosis and ceRNA network of NCBP2 were evaluated and constructed.

2.1. Data acquisition

Transcriptome data and clinical information relevant to 374 patients with HCC were obtained from the TCGA database. With the

Table 1
Clinical information of 365 LIHC samples in TCGA database.

Feature	Train cohort (n = 184)		Test cohort (n = 181)		Entire cohort (n = 365)	
	n	%	n	%	n	%
Age						
≤65	113	61.4	114	63.0	227	62.2
>65	71	38.6	67	37.0	138	37.8
Gender						
Female	55	29.9	64	35.4	119	32.6
Male	129	70.1	117	64.6	246	67.4
Grade						
G1	28	15.2	27	14.9	55	15.1
G2	89	48.4	86	47.5	175	47.9
G3	59	32.1	59	32.6	118	32.3
G4	5	2.7	7	3.9	12	3.3
Unknown	3	1.6	2	1.1	5	1.4
Stage						
Stage I	82	44.6	88	48.6	170	46.6
Stage II	42	22.8	42	23.2	84	23.0
Stage III	47	25.5	36	19.9	83	22.7
Stage IV	1	0.5	3	1.7	4	1.1
Unknown	12	6.5	12	6.6	24	6.6
T classification						
T1	87	47.3	93	51.4	180	49.3
T2	45	24.5	46	25.4	91	24.9
T3	43	23.4	35	19.3	78	21.4
T4	8	4.3	5	2.8	13	3.6
Unknown	1	0.5	2	1.1	3	0.8
M classification						
M0	134	72.8	129	71.3	263	72.1
M1	1	0.5	2	1.1	3	0.8
Unknown	49	26.6	50	27.6	99	27.1
N classification						
N1	127	69.0	121	66.9	248	67.9
N2	1	0.5	3	1.7	4	1.1
Unknown	55	29.9	57	31.5	113	31.0

exclusion of patients without survival information, 365 HCC subjects were included in the modeling. Then, we randomly and evenly allocated these 365 patients into the training cohort (n = 184) and test cohort (n = 181). The baseline data of patients involved in constructing the prognosis model is presented in Table 1. Radiosensitivity-related genes were gained from the dbCRSR database, and 385 genes were detected in HCC (Supplementary Table S1). M7G-related genes were derived from the literature, and MSigDB database [15], and 40 genes were expressed in HCC (Supplementary Table S2).

2.2. Screening of m7G- and radiosensitivity-associated genes

First, the association between m7G-related genes and radiosensitivity-related genes was analyzed using |r|>0.5, $p < 0.05$ as the standard. Then, we screened the prognostic genes by univariate analysis of these candidate genes (|HR|>1.0, P < 0.05). M7G-related differentially expressed genes (DEGs) were screened by p < 0.05 and |log2FC|≥1 criteria. We identified the m7G-related differentially expressed genes (DEGs) based on $p < 0.05$ and |log2FC|≥1. A veen map was used to show the intersection of genes with prognosis and differential expression. PPI network of intersection genes was constructed using the STRING website [16]. Cytoscape plug-in cyto-Hubba was used to determine the hub gene in the PPI network.
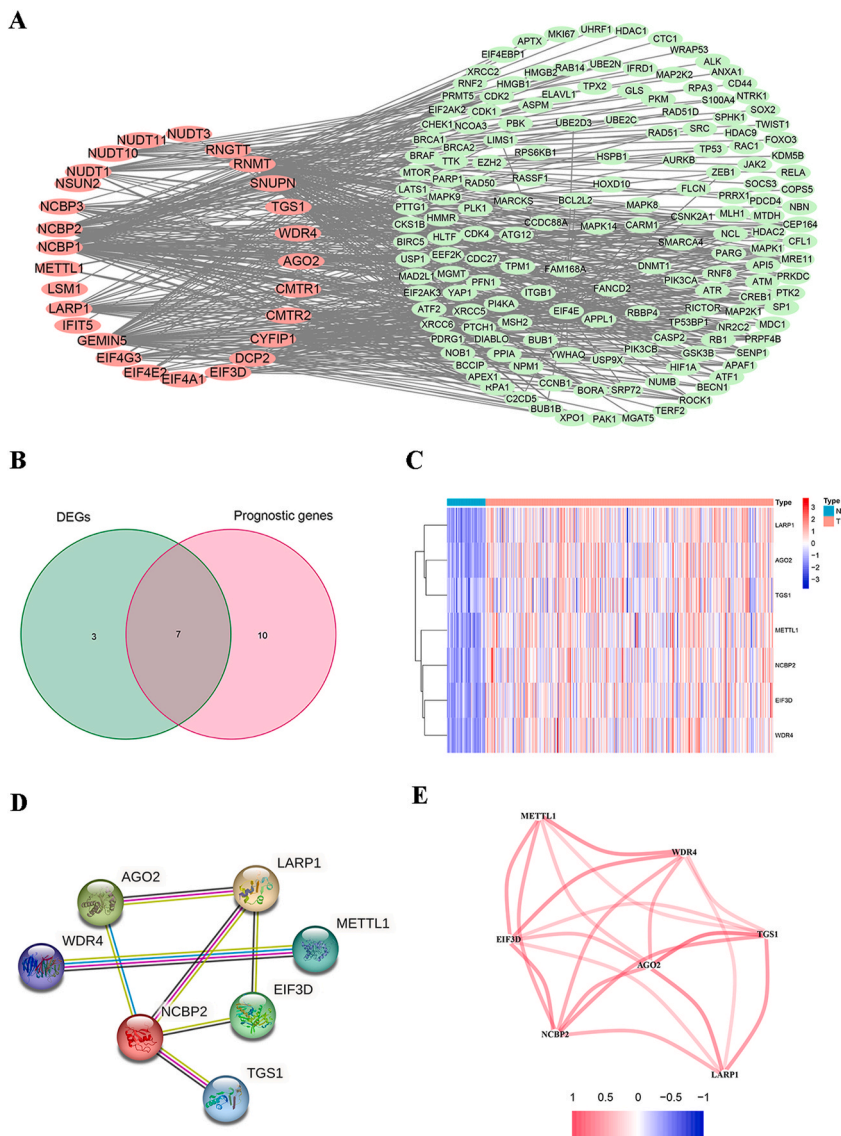

Fig. 1. Identification of radiosensitivity- and m7G-associated genes. A The correlation between 164 radiosensitivity-related genes and 28 m7G-related genes. B Intersection genes with prognostic value and differential expression. C Heatmap of the expression levels of 7 intersection genes. D The PPI network of 7 intersection genes. E Correlation network of 7 intersection genes.
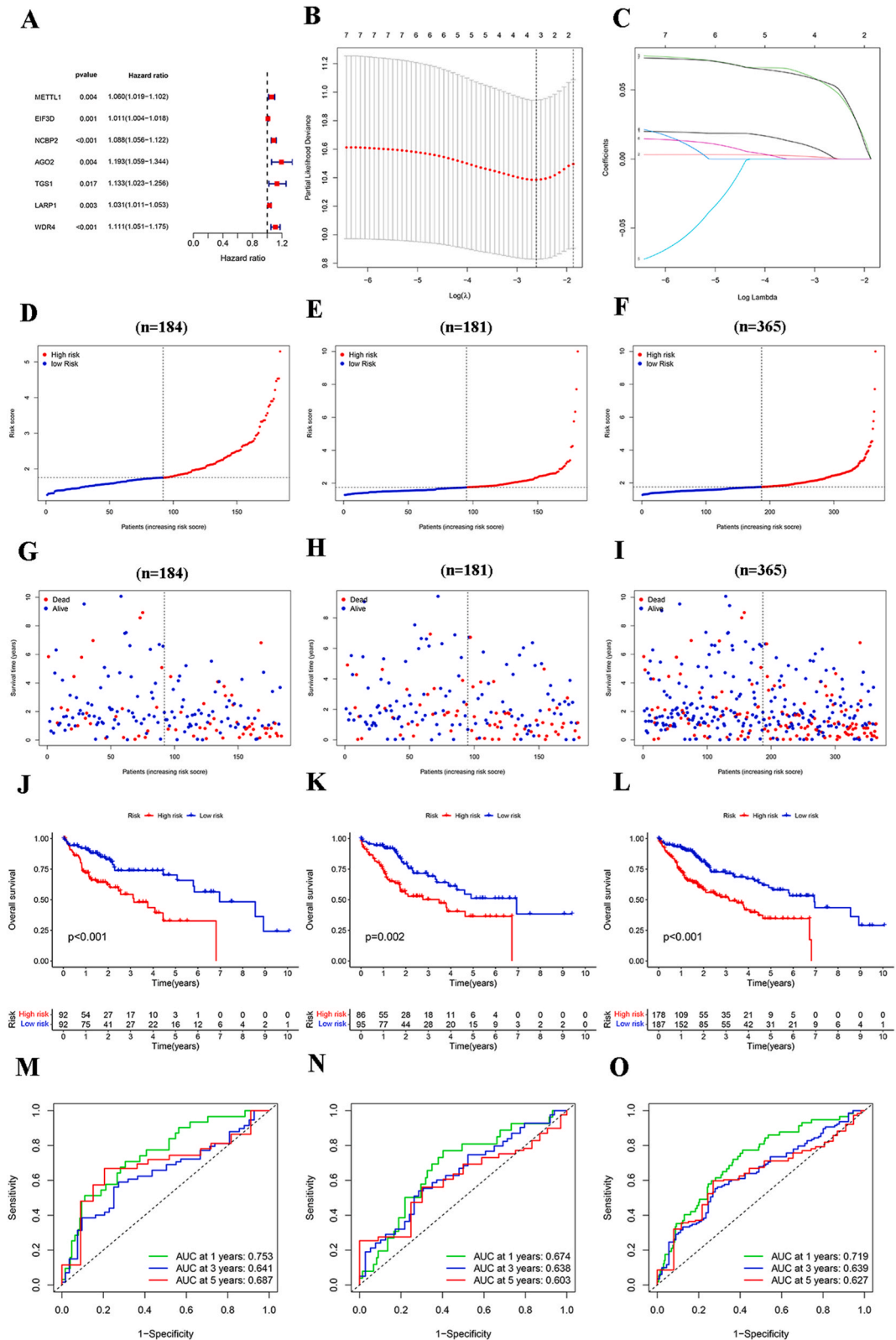
(caption on next page)

Fig. 2. Construction and assessment of the prognostic model. A Univariate Cox regression analysis of 7 intersection genes. **B–C** LASSO regression analysis. **D-F** Risk score distribution of train set (D), test set (E), and entire TCGA set (F). **G-I** survival status scatterplot of train set (G), test set (H), and entire TCGA set (I). **J-L** Kaplan-Meier analysis of train set (J), test set (K), and entire TCGA set (L). **M-O** ROC curve of train set (M), test set (N), and entire TCGA set (O).

2.3. Construction and evaluation of the prognostic model

The prognosis model was constructed by LASSO (least absolute shrinkage and selection operator) regression and validated by test cohort set and total TCGA-LIHC set. The risk score was equal to the gene expression level multiplied by the coefficient of the corresponding gene. We adopt the Kaplan-Meier (KM) method, receiver operating characteristic (ROC), principal component analysis (PCA), and t-distributed stochastic neighbor embedding (*t*-SNE) to assess the prognosis efficiency and predictive ability of the model.

2.4. Nomogram construction

We used "ggDCA" and "timeROC" packages to construct a nomogram based on risk scores and related clinical data. Relevant clinical data include age, sex, stage, grade, and T, N classification of HCC patients.

2.5. Immune cell infiltration, immunotherapy, and drug sensitivity

We assessed the difference in immune infiltrates between different risk groups using TIMER, CIBERSORT, CIBERSORT-ABS, QUANTISEQ, MCPCOUNTER, XCELL, and EPIC. Immune function was evaluated by calculating the infiltration score of immune cells with "GSVA" and "GSEABase" software packages.

Immunotherapy scores were downloaded from the TCIA database (https://tcia.at).

The "oncoPredict" package was utilized to compare the sensitivity differences of commonly used chemotherapeutics for HCC between various risk groups. Drug-sensitive data derived from Genomics of Drug Sensitivity in Cancer (GDSC).

2.6. Upstream miRNAs and lncRNAs predication

StarBase database was adapted to forecast the upstream miRNAs and lncRNAs. StarBase included seven prediction platforms (TargetScan, PicTar, miRanda, microT, miRmap, RNA22, and PITA) [17]. MiRNAs or lncRNAs appearing in more than two programs were defined as upstream miRNAs or lncRNAs.

2.7. Statistical analysis

R 4.2.1 is used in the whole statistical analysis. Wilcoxon test and student's t-test were used for continuous variables. P value < 0.05 indicates statistical significance.

3. Results

3.1. Identification of m7G- and radiosensitivity-associated genes with prognostic value and differential expression

Correlation analysis showed that 28 m7G-related genes were strongly correlated with 164 radiosensitivity-related genes (Fig. 1A). Univariate Cox analysis indicated that 17 m7G-related genes had prognostic values (Supplementary Table S3). Besides, 10 DEGs were obtained by comparing the expression differences of 40 m7G-related genes between HCC and normal samples. Veen map showed that seven overlapping genes (METTL1, EIF3D, NCBP2, AGO2, TGS1, LARP1, WDR4) had prognostic value and differential expression (Fig. 1B). Moreover, the expression of 7 overlapping genes increased (Fig. 1C). The protein-protein interaction (PPI) network of overlapping genes was established by the string website (Fig. 1D). Meanwhile, overlapping genes were positively correlated (Fig. 1E).

3.2. Construction and assessment of the prognostic model

Univariate Cox regression indicated that all overlapping genes were related to OS (Fig. 2A). Through LASSO Cox regression analysis, METTL1, EIF3D, NCBP2, and WDR4 were selected from the overlapping genes to construct the prognosis model (Fig. 2B and C). At the same time, some studies have reported the effects of these genes on HCC. METTL1 might lead to poor prognosis in HCC patients [18]. WDR4 can be combined with METTL1 to form a methyltransferase complex, which further affects the prognosis of HCC patients [19,20]. EIF3D is considered to be a novel biomarker that facilitates the HCC progression [21]. In addition, several articles have also indicated that NCBP2 is a promising prognostic biomarker [22,23]. The risk score of HCC patients in each set is calculated according to the following risk score formula: (METTL1*0.000835638872508109)+(EIF3D*0.000528025128133416)+ (NCBP2*0.0500104100164452)+(WDR4*0.0532257256903693).

Patients whose scores are higher than the median risk score are classified into high-risk group, and vice versa (Fig. 2D, E, F). The survival status scatterplot showed that the survival time of patients was shortened with the increase in risk score (Fig. 2G, H, I). In all

cohorts, the prognosis of the high-risk group is worse than that of the low-risk group (Fig. 2J–L). The result of the ROC curve implied that our model had an ideal prediction efficiency (Fig. 2M–O). PCA and *t*-SNE results manifested that high and low-risk groups could significantly differentiate HCC patients (Supplementary Figure S2, B).

3.3. Correlation between prognostic model and clinical parameters

In the whole TCGA-LIHC, univariate (Supplementary Figure S2C, p < 0.001) and multivariate (Supplementary Figure S2D, p <
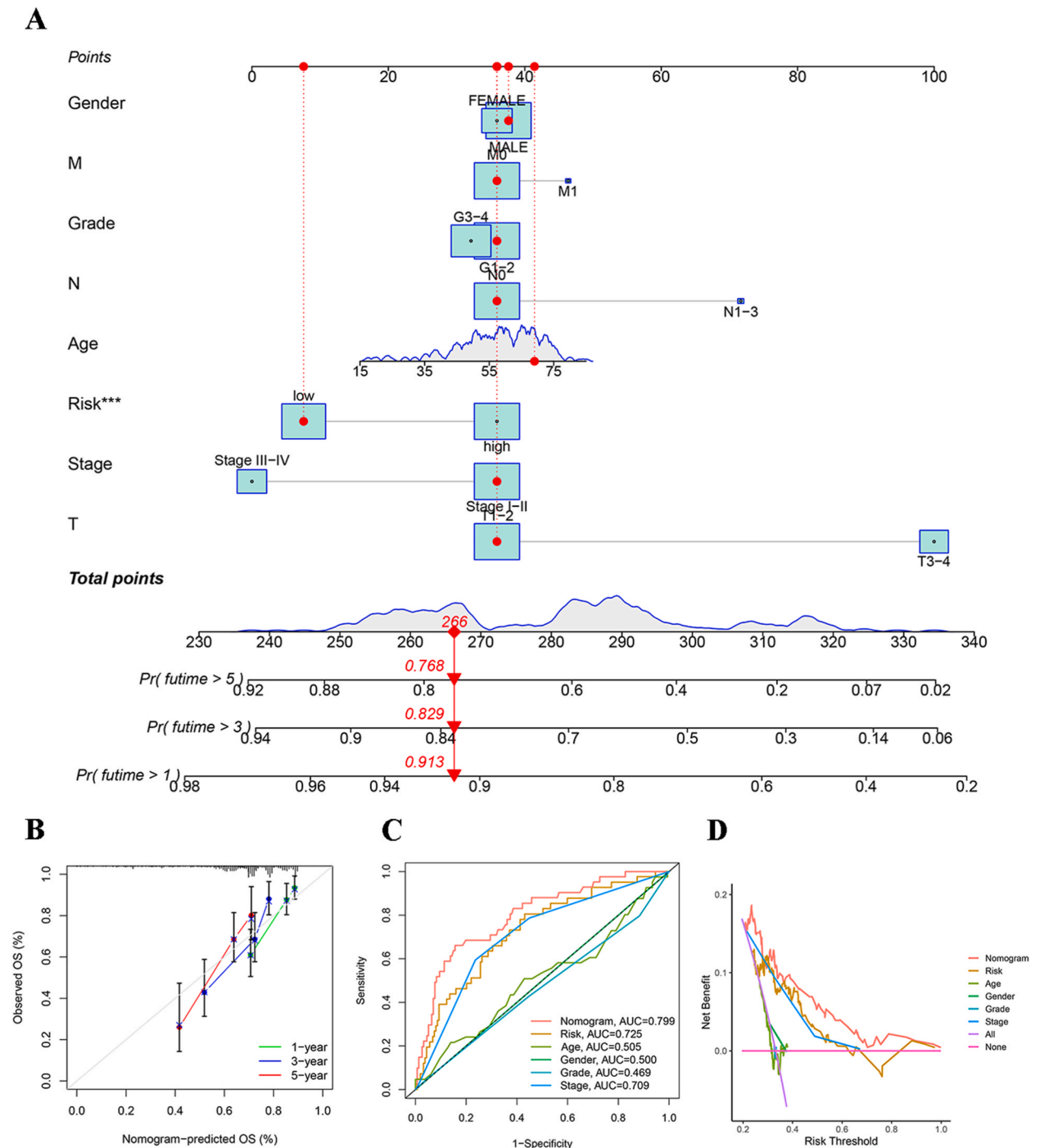

Fig. 3. Nomogram construction. A Nomogram. **B-D** Calibration curve (B), and ROC curve (C), DCA analysis (D) of the nomogram.
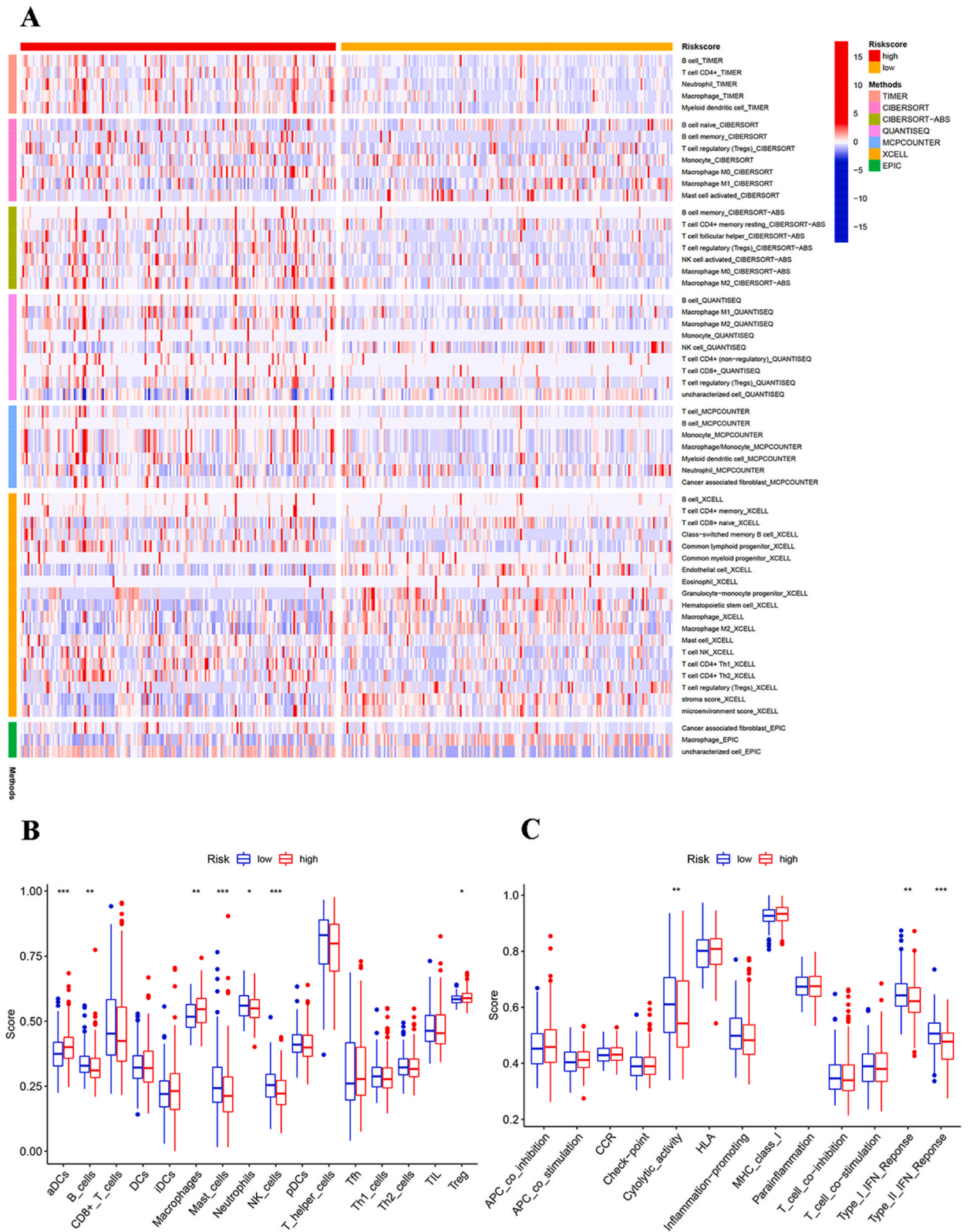
Fig. 4. Immune features and drug sensitivity. A Heatmap of immune cell infiltration based on seven analytic methods. B–C of immune cell infiltration (B) and immune function (C) analysis in two risk groups using ssGSEA. D drug sensitivity analysis in two risk groups.
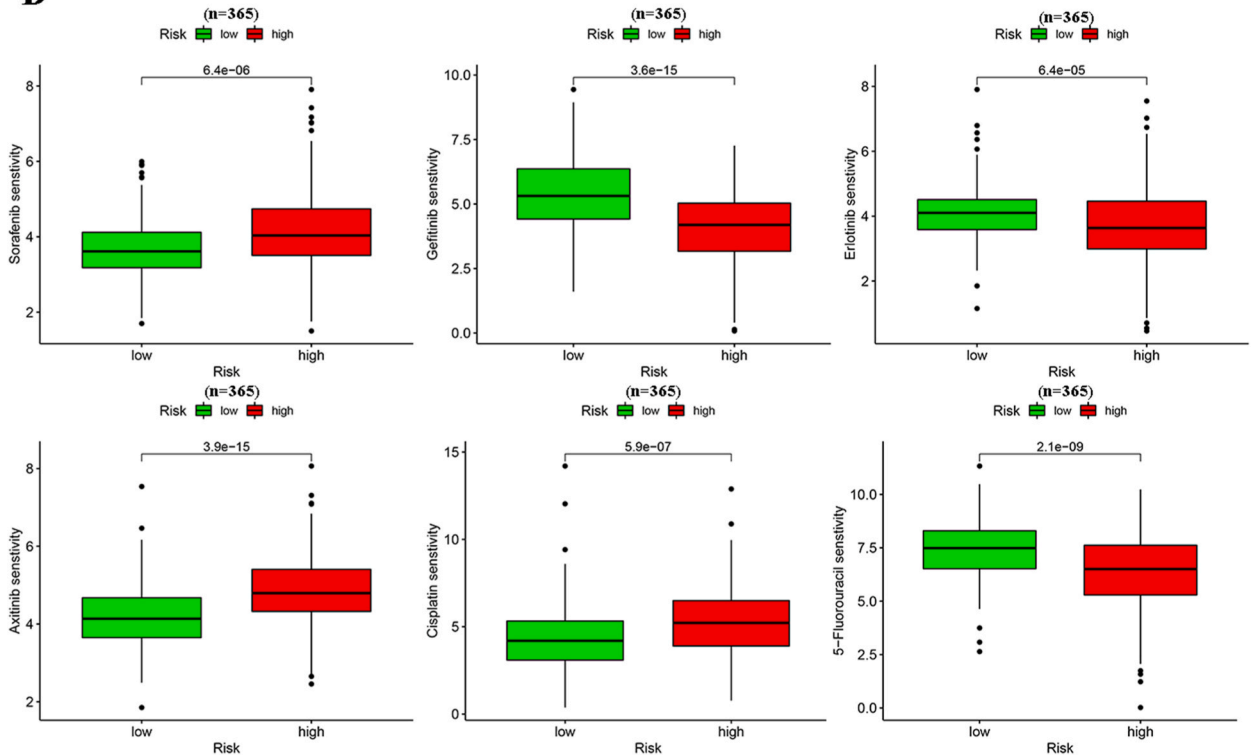
Fig. 4. (*continued*).

0.001) Cox regression indicated that risk score could be used as an independent prognostic factor of OS. Besides, the risk score was associated with other risk factors of age ($p = 0.004$), grade ($p < 0.001$), and T classification ($p = 0.016$) but not with gender, N classification, and M classification (Supplementary Figure S2E-K). In order to better evaluate the 1-, 3-and 5-year survival of HCC patients, a nomogram based on risk score and other risk factors was constructed (Fig. 3A). The predicted OS of the nomogram presented a high consistency with the actual OS (Fig. 3B). Besides, the prediction efficiency of the nomogram and risk value is better than other risk indicators (Fig. 3C and D).

3.4. Function and pathway enrichment analysis

Then, we applied the GSEA to explore the potentially different biological pathways in different risk groups. GSEA analysis indicated cell cycle, dilated cardiomyopathy, ECM receptor interaction, neuroactive ligand-receptor interaction, and ribosome enrichment in a high-risk group (Supplementary Figure S3A). Meanwhile, complement and coagulation cascades, drug metabolism cytochrome P450, fatty acid metabolism, retinol metabolism, and steroid hormone biosynthesis were enriched in the low-risk group (Supplementary Figure S3B). In addition, we performed GO and KEGG analysis on DEGs in different risk groups. Functions of DEGs were mainly enriched in nuclear division, chromosome segregation, and mitotic nuclear division (Supplementary Figure S3C). Pathways of DEGs were enriched in the cell cycle, ECM receptor interaction, protein digestion and absorption, and metabolism of xenobiotics by cytochrome P450 (Supplementary Figure S3D).

3.5. Immune features and drug sensitivity

Fig. 4A presentsthe results of immune infiltration among different risk groups obtained by seven analytical methods. The results indicated that the infiltration of most immune cells in the high-risk group, such as T cells and macrophages, was more prominent. ssGSEA analyzed the differences in immune status and immune function in different risk groups. ADC, macrophages, and Treg infiltrated obviously in the high-risk group. B cells, mast cells, neutrophils, and NK cells were more expressed in the low-risk group (Fig. 4B). Besides, the cytolytic activity, type I IFN, and type II IFN reactions were more significant in the low-risk group (Fig. 4C). Then, we selected the commonly used therapeutic drugs for HCC and compared the differences in drug sensitivity among different risk groups. Sorafenib, erlotinib, cisplatin, and axitinib had better effects in the low-risk group, while gefitinib and 5-fluorouracil had better effects in the high-risk group (Fig. 4D).
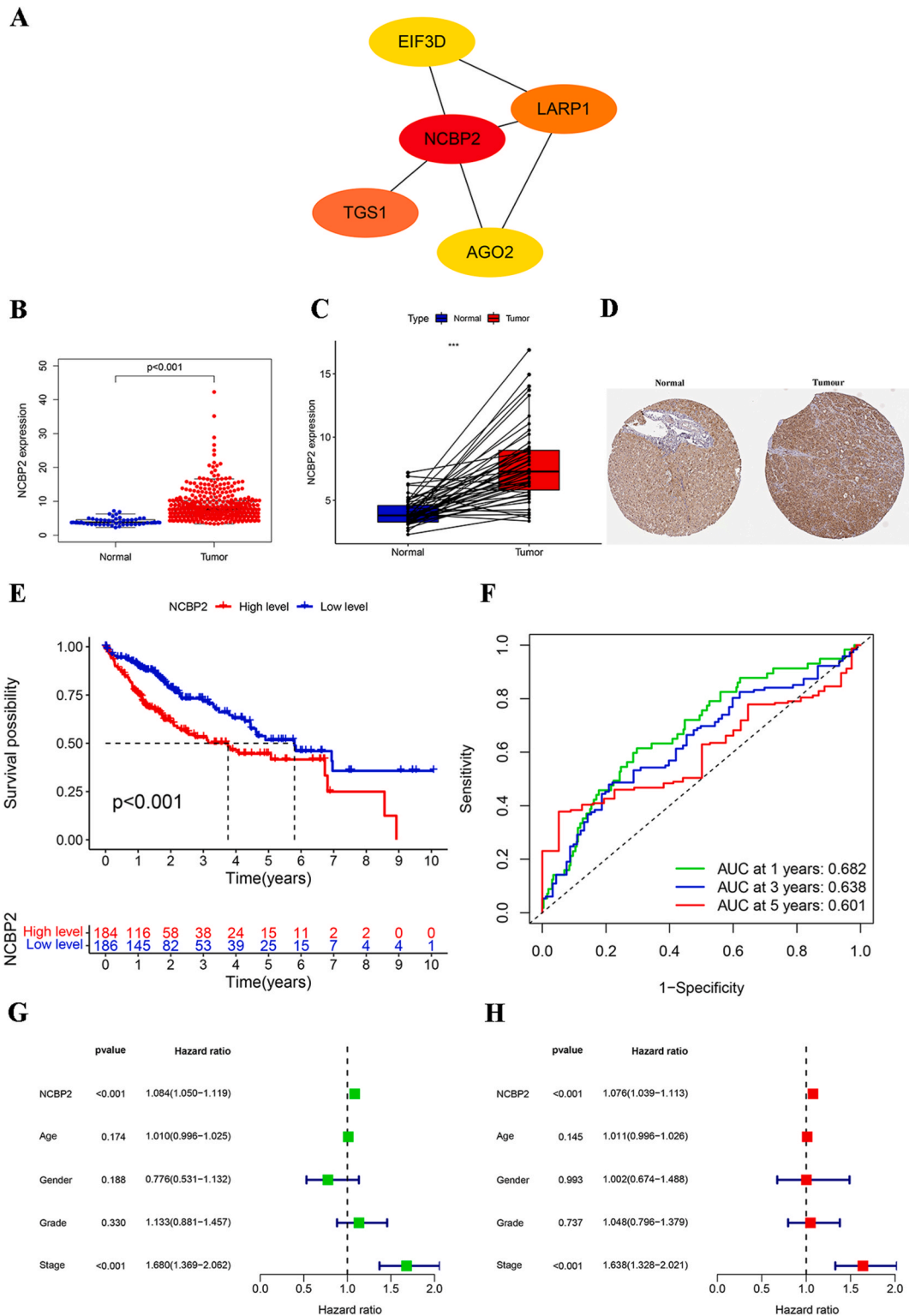
Fig. 5. Expression of NCBP2 and its prognostic value. A Hub gene in the PPI network with a score of >2. B Expression of NCBP2 in tumor samples and normal samples. C Expression of NCBP2 in tumor samples and matched normal samples. D Immunohistochemical staining results of NCBP2 in normal liver and liver cancer tissues were obtained from the HPA database. E Kaplan–Meier analysis for NCBP2. F ROC curve for NCBP2. G-H Univariate (G) and multivariate (H) Cox regression analysis of NCBP2 expression and clinical parameters.
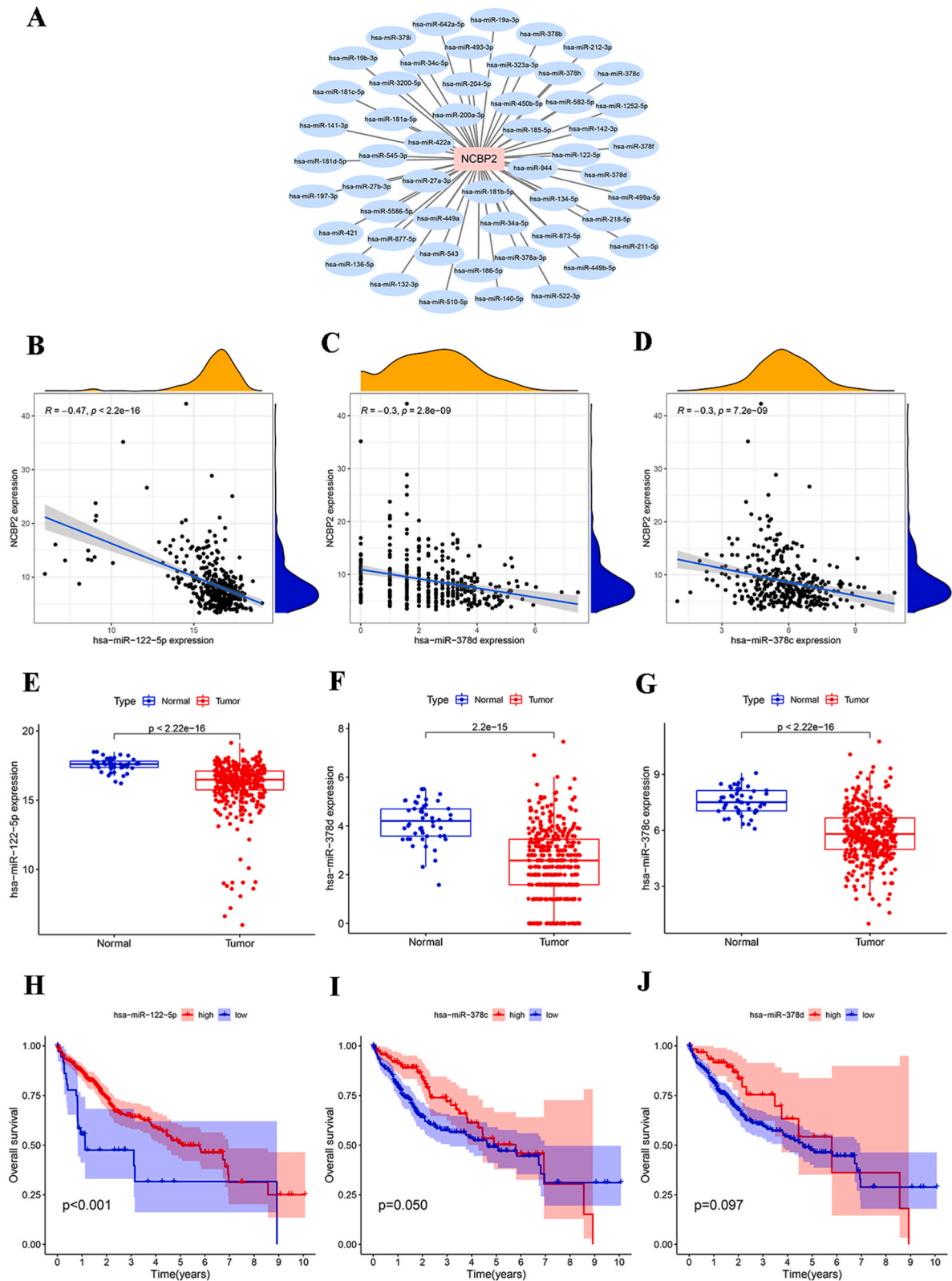
Fig. 6. Identification of upstream miRNAs of NCBP2. A The miRNA-NCBP2 regulatory network. **B-D** Correlation analysis between NCBP2 and miR-122-5p (B), miR-378d (C), and miR-378c (D). **E-G** The expression of miR-122-5p (E), miR-378d (F), and miR-378c (G). **H-J** Kaplan–Meier analysis for miR-122-5p (H), miR-378d (I), and miR-378c (J).

3.6. Expression of NCBP2 and its prognostic value

Using Cytoscape to screen the intersection of genes related to prognosis and differentially expressed, NCBP2 was found to be the hub gene (Fig. 5A). NCBP2 binds to NCBP1 to form a nuclear cap-binding complex associated with RNA polymerase II transcripts [24]. Studies have shown that NCBP2 is an oncogene [22]. NCBP2 was upregulated in HCC (Fig. 5B). The result was similar to that of matched normal samples (Fig. 5C). Results from the IHC of the HPA database indicated an up-regulation of NCBP2 protein levels in HCC tissues (Fig. 5D).

Next, survival analysis for NCBP2 in HCC showed that patients with high NCBP2 expression had a worse prognosis (Fig. 5E). The ROC curve manifested that NCBP2 possessed a tremendous prognostic value in 1, 3, and 5 years (Fig. 5F). Univariate and multivariate COX regression indicated that NCBP2 had independent prognostic value (Fig. 5G and H).

3.7. NCBP2 related genes and the correlation between NCBP2 and immunotherapy

We evaluated the correlation between NCBP2 and m7G- and radiosensitivity-associated genes. Supplementary Figure S4A displayed the top 10 m7G- and radiosensitivity-associated genes related to NCBP2. Then, we explored the relationship between NCBP2 and 31 immune checkpoint genes, which were significantly positively related to NCBP2, especially CD26 and TNFSF15 (Supplementary Figure S4B). The NCBP2 low-expression group showed remarkable effects on anti-CTLA4, anti-PD1, and combination treatment (Supplementary Figure S4C-F).

3.8. Prediction and assessment of upstream miRNAs of NCBP2

The starbase database predicted 52 upstream miRNAs that might bind to NCBP2 and we visualized the results using Cytoscape software (Fig. 6A). Next, we analyzed the correlation between 52 miRNAs and NCBP2 and found that miR-122-5p, miR-378d, and miR-378c were significantly and negatively correlated with NCBP2 (Fig. 6B–D). MiR-122-5p, miR-378d, and miR-378c were downregulated in HCC (Fig. 6E–G). Besides, KM analysis indicated that the downregulation of miR-122-5p was related to the poor prognosis of HCC patients (Fig. 6H–J). So, miR-122-5p is probably the most promising regulatory miRNA for NCBP2.

3.9. Prediction and assessment of upstream lncRNAs of miR-122-5p and construction of ceRNA network

We still used the starbase database to predict the lncRNAs of miR-122-5p and eventually obtained 77 upstream lncRNAs of miR-122-5p (Supplementary Figure S5. Then, we analyzed the correlation between these 77 lncRNAs and miR-122-5p. At last, 23 lncRNAs, which were up-regulated and negatively correlated with miR-122-5p in patients with HCC, were obtained (Supplementary Table S4). At the same time, these 23 lncRNAs were positively correlated with NCBP2 (Supplementary Table S5). The survival results of 23 lncRNAs showed that the high expression of LINC00205, Z97832.2, AL358472.3, AC145423.2, LINC00909, LINC00294, SNHG7, NUTM2B-AS1, LINC01278 and AC096992.2 predicted a shorter survival time (Supplementary Figure S5B-K). The ceRNA regulatory network that NCBP2 may participate in is shown in Supplementary Figure S6.

4. Discussion

Given radiotherapy's critical role in treating patients with HCC, exploring the mechanisms of radioresistance and increasing radiosensitivity remains a clinically pressing concern [25,26]. The modification mechanism of m7G is intricate and regulated by diverse factors, are closely related to tumorigenesis [27,28]. Recent studies have shown that m7G-related genes could affect radioresistance and prognosis after radiotherapy [14,29]. However, whether m7G-related genes will affect radiosensitivity has yet to be reported. In this study, we identified the m7G- and radiosensitivity-associated genes. Seven genes with differential expression and prognostic value were screened out, including METTL1, EIF3D, NCBP2, AGO2, TGS1, LARP1, and WDR4.

The prognostic model was established based on METTL1, EIF3D, NCBP2, and WDR4. Our model performed excellently in predicting HCC prognosis. HCC patients could be distinguished into two different risk groups in line with the risk score of our model. The low-risk group has a better prognosis. The risk score has an excellent ability to predict OS independently and was relevant to clinical features of age, grade, and T classification. In addition, we established a nomogram integrating risk scores with clinical signs to explore clinical application values further.

Different enrichment of pathways between two risk groups may be one of the reasons for different prognosis outcomes. CYP-mediated drug metabolism, fatty acid metabolism, retinol metabolism, and steroid hormone biosynthesis were mainly activated in the low-risk group. Multiple studies have shown that fatty acid, retinol metabolism, and steroid hormone biosynthesis are promising anticancer strategies [30–32]. Interestingly, drug sensitivity analysis indicated that low-risk patients were susceptible to sorafenib, and CYP1A2 can improve the therapeutic effect of sorafenib on HCC by inhibiting the NF-κB p65 axis [32].

The immune microenvironment plays an essential role in the tumors. Tumor-associated macrophages accelerate the progression of HCC [33]. TANs promote HCC development by recruiting macrophages and Treg cells [34]. In the high-risk group, macrophages and Treg cells infiltrated more. A high cytolytic activity score means better immunogenicity and prognosis [35]. Besides, interferon I and II reactions are reported to be involved in the antitumor process [36,37]. Cytolytic activity, interferon I and II reactions were significantly activated in a low-risk group. The discrepancy in immune infiltration between the different risk groups may be a potential mechanism for different prognostic outcomes.

To further explore the relationship and potential biological mechanism behind the intersection genes, we screened out the hub gene, NCBP2. NCBP2 can independently predict OS and could lead to a poor prognosis of HCC. Immune checkpoints, such as CD26 and TNFSF15, were strongly correlated with NCBP2, and patients with low expression of NCBP2 were sensitive to anti-CTLA4 therapy, anti-PD-1 therapy, and combination therapy. NCBP2 may have a particular guiding significance for the immunotherapy of HCC patients.

Increasing evidence reports that the ceRNA network is involved in tumorigenesis, including HCC [38]. We utilized the Starbase database, expression analysis, correlation analysis, and survival analysis to find and evaluate the upstream miRNA of NCBP2. MiR-122-5p, as a candidate miRNA, can be used as a tumor suppressor and is beneficial to the prognosis of HCC patients. Several studies have indicated that miR-122-5p restrains CLIC1-induced HCC progression and targets LDHA to inhibit glycolysis of HCC cells [39,40]. The upstream lncRNAs of miR-122-5p/NCBP2 axis were also predicted and assessed, including LINC00205, Z97832.2, AL358472.3, AC145423.2, LINC00909, LINC00294, SNHG7, NUTM2B-AS1, LINC01278 and AC096992.2. These ten lncRNAs were upregulated in HCC and predicted poor prognosis. LINC00205 and SNHG7 have been confirmed to accelerate the progression of HCC and target miR-122-5p [41,42]. It has been reported that LINC01278 participates in tumorigenesis by affecting miR-1258 expression [43]. The ceRNA regulatory network we constructed provides a new direction for the latent regulatory mechanisms of HCC.

There are still some limitations. Firstly, all data sets were derived from public databases without experimental verification. Future rigorous experimental verification will further strengthen the persuasion of our conclusion. Secondly, some patients' N and M classification data were difficult to acquire. The acquisition of more and better clinical characteristic data will make our conclusion more reliable.

5. Conclusion

The prognosis model of m7G- and radiosensitivity-related genes is constructed, and widely used in clinical prognosis, immunotherapy, and drug therapy. NCBP2, as a hub gene, may be a prognostic biomarker for HCC and is related to immunotherapy. Establishing the NCBP2/miR-122-5p axis helps study the mechanism of ceRNA and provides new ideas for finding a new candidate biomarker.

Availability of data and material

The datasets analyzed in this study came from TCGA (https://portal.gdc.cancer.gov/repository).

Funding

CRediT authorship contribution statement

Miaowen Liu: Writing – original draft, Software, Methodology, Investigation, Data curation, Conceptualization. **Meiyan Zhu:** Writing – original draft, Methodology, Formal analysis, Data curation, Conceptualization. **Yingxiong Huang:** Supervision, Project administration, Investigation, Data curation. **Jian Wu:** Writing – review & editing, Supervision, Resources, Methodology. **Zhenwei Peng:** Writing – review & editing, Validation, Supervision, Project administration, Investigation, Formal analysis. **Ying Liang:** Writing – review & editing, Visualization, Supervision, Project administration, Funding acquisition, Data curation.

Declaration of competing interest

The authors have no conflicts of interest to declare.

Acknowledgements

Appendix A. Supplementary data

Supplementary data to this article can be found online at https://doi.org/10.1016/j.heliyon.2024.e29925.

References

[1] H. Sung, et al., Global cancer statistics 2020: GLOBOCAN estimates of incidence and mortality worldwide for 36 cancers in 185 countries, CA Cancer J Clin 71 (3) (2021) 209–249.

[2] J.D. Yang, et al., A global view of hepatocellular carcinoma: trends, risk, prevention and management, Nat. Rev. Gastroenterol. Hepatol. 16 (10) (2019) 589–604.

[3] EASL clinical practice guidelines: management of hepatocellular carcinoma, J. Hepatol. 69 (1) (2018) 182–236.

[4] L. Jia, et al., HBV induced hepatocellular carcinoma and related potential immunotherapy, Pharmacol. Res. 159 (2020) 104992.

[5] N. Ganne-Carrié, P. Nahon, Hepatocellular carcinoma in the setting of alcohol-related liver disease, J. Hepatol. 70 (2) (2019) 284–293.

[6] E.E. Powell, V.W. Wong, M. Rinella, Non-alcoholic fatty liver disease, Lancet 397 (10290) (2021) 2212–2224.

[7] L. Kulik, H.B. El-Serag, Epidemiology and management of hepatocellular carcinoma, Gastroenterology 156 (2) (2019) 477–491.e1.

[8] T. Meyer, Stereotactic body radiotherapy for hepatocellular carcinoma - still searching for a role, J. Hepatol. 73 (1) (2020) 15–16.

[9] C.Y. Huang, et al., Palbociclib enhances radiosensitivity of hepatocellular carcinoma and cholangiocarcinoma via inhibiting ataxia telangiectasia-mutated kinase-mediated DNA damage response, Eur. J. Cancer 102 (2018) 10–22.

[10] M. Yang, et al., COMMD10 inhibits HIF1α/CP loop to enhance ferroptosis and radiosensitivity by disrupting Cu-Fe balance in hepatocellular carcinoma, J. Hepatol. 76 (5) (2022) 1138–1150.

[11] D. Wiener, S. Schwartz, The epitranscriptome beyond m(6)A, Nat. Rev. Genet. 22 (2) (2021) 119–131.

[12] Y. Luo, et al., The potential role of N(7)-methylguanosine (m7G) in cancer, J. Hematol. Oncol. 15 (1) (2022) 63.

[13] M. Huang, et al., METTL1-Mediated m7G tRNA modification promotes lenvatinib resistance in hepatocellular carcinoma, Cancer Res. 83 (1) (2023) 89–102.

[14] J. Liao, et al., Methyltransferase 1 is required for nonhomologous end-joining repair and renders hepatocellular carcinoma resistant to radiotherapy, Hepatology 77 (6) (2023) 1896–1910.

[15] A. Liberzon, et al., Molecular signatures database (MSigDB) 3.0, Bioinformatics 27 (12) (2011) 1739–1740.

[16] D. Szklarczyk, et al., The STRING database in 2023: protein-protein association networks and functional enrichment analyses for any sequenced genome of interest, Nucleic Acids Res. 51 (D1) (2023) D638–d646.

[17] J.H. Li, et al., starBase v2.0: decoding miRNA-ceRNA, miRNA-ncRNA and protein-RNA interaction networks from large-scale CLIP-Seq data, Nucleic Acids Res. 42 (Database issue) (2014) D92–D97.

[18] E.A. Orellana, et al., METTL1-mediated m(7)G modification of Arg-TCT tRNA drives oncogenic transformation, Mol Cell 81 (16) (2021) 3323–3338.e14.

[19] Z. Dai, et al., N(7)-Methylguanosine tRNA modification enhances oncogenic mRNA translation and promotes intrahepatic cholangiocarcinoma progression, Mol Cell 81 (16) (2021) 3339–3355.e8.

[20] Z. Chen, et al., METTL1 promotes hepatocarcinogenesis via m(7) G tRNA modification-dependent translation control, Clin. Transl. Med. 11 (12) (2021) e661.

[21] T. Li, et al., Transcriptomic analyses of RNA-binding proteins reveal eIF3c promotes cell proliferation in hepatocellular carcinoma, Cancer Sci. 108 (5) (2017) 877–885.

[22] K. Zhou, et al., N7-Methylguanosine regulatory genes profoundly affect the prognosis, progression, and antitumor immune response of hepatocellular carcinoma, Front Surg 9 (2022) 893977.

[23] Y. Zhao, T. Huang, P. Huang, Integrated analysis of tumor mutation burden and immune infiltrates in hepatocellular carcinoma, Diagnostics 12 (8) (2022).

[24] Y. Dou, et al., NCBP3 positively impacts mRNA biogenesis, Nucleic Acids Res. 48 (18) (2020) 10413–10427.

[25] N. Ohri, et al., Radiotherapy for hepatocellular carcinoma: new indications and directions for future study, J Natl Cancer Inst 108 (9) (2016).

[26] A.M. Buckley, et al., Targeting hallmarks of cancer to enhance radiosensitivity in gastrointestinal cancers, Nat. Rev. Gastroenterol. Hepatol. 17 (5) (2020) 298–313.

[27] A. Alexandrov, M.R. Martzen, E.M. Phizicky, Two proteins that form a complex are required for 7-methylguanosine modification of yeast tRNA, Rna 8 (10) (2002) 1253–1266.

[28] C. Enroth, et al., Detection of internal N7-methylguanosine (m7G) RNA modifications by mutational profiling sequencing, Nucleic Acids Res. 47 (20) (2019) e126.

[29] X. Zeng, et al., Eliminating METTL1-mediated accumulation of PMN-MDSCs prevents hepatocellular carcinoma recurrence after radiofrequency ablation, Hepatology 77 (4) (2023) 1122–1138.

[30] C. Qin, et al., Metabolism of pancreatic cancer: paving the way to better anticancer strategies, Mol. Cancer 19 (1) (2020) 50.

[31] S.M. Jeon, E.A. Shin, Exploring vitamin D metabolism and function in cancer, Exp. Mol. Med. 50 (4) (2018) 1–14.

[32] J.A. Kim, J.H. Jang, S.Y. Lee, An updated comprehensive review on vitamin A and carotenoids in breast cancer: mechanisms, genetics, assessment, current evidence, and future clinical implications, Nutrients 13 (9) (2021).

[33] D. Bao, et al., Mitochondrial fission-induced mtDNA stress promotes tumor-associated macrophage infiltration and HCC progression, Oncogene 38 (25) (2019) 5007–5020.

[34] S.L. Zhou, et al., Tumor-associated neutrophils recruit macrophages and T-regulatory cells to promote progression of hepatocellular carcinoma and resistance to sorafenib, Gastroenterology 150 (7) (2016) 1646–1658.e17.

[35] H. Takahashi, et al., Immune cytolytic activity for comprehensive understanding of immune landscape in hepatocellular carcinoma, Cancers 12 (5) (2020).

[36] L. Zitvogel, et al., Type I interferons in anticancer immunity, Nat. Rev. Immunol. 15 (7) (2015) 405–414.

[37] G.P. Dunn, C.M. Koebel, R.D. Schreiber, Interferons, immunity and cancer immunoediting, Nat. Rev. Immunol. 6 (11) (2006) 836–848.

[38] H. Wang, et al., STAT3-mediated upregulation of lncRNA HOXD-AS1 as a ceRNA facilitates liver cancer metastasis by regulating SOX4, Mol. Cancer 16 (1) (2017) 136.

[39] X. Jiang, et al., Up-regulation of CLIC1 activates MYC signaling and forms a positive feedback regulatory loop with MYC in Hepatocellular carcinoma, Am. J. Cancer Res. 10 (8) (2020) 2355–2370.

[40] X. Wang, P. Zhang, K. Deng, MYC promotes LDHA expression through MicroRNA-122-5p to potentiate glycolysis in hepatocellular carcinoma, Anal. Cell Pathol. 2022 (2022) 1435173.

[41] L. Zhang, et al., LINC00205 promotes proliferation, migration and invasion of HCC cells by targeting miR-122-5p, Pathol. Res. Pract. 215 (9) (2019) 152515.

[42] X. Yang, et al., LncRNA SNHG7 accelerates the proliferation, migration and invasion of hepatocellular carcinoma cells via regulating miR-122-5p and RPL4, Biomed. Pharmacother. 118 (2019) 109386.

[43] W.J. Huang, et al., The β-catenin/TCF-4-LINC01278-miR-1258-Smad2/3 axis promotes hepatocellular carcinoma metastasis, Oncogene 39 (23) (2020) 4538–4550.